Heat Transfer and the Mechanism of Drying in Agitation Fluidized Bed

Satoru WATANO,* Nan YEH, and Kei MIYANAMI

Department of Chemical Engineering, Osaka Prefecture University, 1–1 Gakuen-cho, Sakai, Osaka, 599–8531 Japan.
Received January 27, 1999; accepted April 1, 1999

This paper describes experimental and numerical analyses on the heat transfer between air and particles in an agitation fluidized bed drying process. Spherical particles made of crystalline cellulose having been dampened to 15% were dried in an agitation fluidized bed. The effects of the operating variables such as air temperature, air velocity, agitator rotational speed and particle size on the heat transfer coefficient between air and particles were investigated experimentally. An empirical equation was then proposed to predict the heat transfer coefficient under various operating variables and particle size. The empirical equation could predict the heat transfer coefficient very accurately.

Key words drying; agitation fluidized bed; heat transfer; prediction

An agitation fluidized bed, defined as a type of fluidized bed equipped with mechanical agitation, has been developed[1—4] and its performance has attracted special interest in powder handling processes. So far, it has been widely used especially in the wet granulation/coating of pharmaceuticals, food and chemical materials, making use of its characteristics that it can reduce segregation by forced circulation and produce spherical and well compacted granules,[3,4] heretofore impossible with a conventional fluidized bed system.[5,6]

However, much attention has been paid on the agitation fluidized bed as a particle drying system. If it is applicable to the drying system, a series of operations such as mixing, granulation/coating and drying processes can be conducted in a single unit, which saves processing time, space and costs and also prevents contamination by dusts.

Up to now, although a lot of research has been carried out on fluidized bed drying,[7—10] there has been no study which focused on the agitation fluidized bed drying. We have just studied the effects of operational variables on the granule properties and drying rate.[11] In order to analyze the performance of the agitation fluidized bed drying in detail, the mechanism of heat transfer between air and particles should be understood.

In this study, agitation fluidized bed drying was carried out using pharmaceutical spherical particles. The effects of operational variables on the heat transfer coefficient between air and particles were investigated. An empirical equation was proposed to predict the heat transfer coefficient between air and particles under various operating variables and particle size.

Experimental

Equipment Figure 1 shows the experimental set-up. An agitation fluidized bed[2,3] (NQ-160, Fuji Paudal Co., Ltd.), equipped with a mechanical agitation blade, was used for the drying experiments. This fluidized bed consisted of two parts: a lower cylindrical vessel (0.160 m in diameter, 0.160 m in depth) and an upper cone vessel tapered 15 degrees (0.80 m in height), both made of stainless steel. An agitator blade turned on a central axis was installed at the bottom of the cylindrical vessel to impart tumbling and circulating motion on the granules. Under the blade, a slit plate was stationed for distributing the fluidization air. The slit plate was composed of five circular plates of different diameters superimposed 0.5 mm apart. Heated air needed for particle fluidization and drying was blown through the slits located between each plate, creating a circulating flow. Fine powders lifted by the fluidizing air were entrapped by bag filters and brushed down by a pulsating jet of air.

The moisture content of particles during the dampening process was measured by an infrared (IR) moisture sensor.[2,3] Feedback control of moisture content was conducted by regulating a liquid feed rate.

Fluidization air velocity was measured by a hot-wire anemometer, which was located at the center of the inlet air duct pipe to detect maximum air velocity. Inlet and outlet air temperatures and humidities were measured by ceramic sensors.

Main operational variables such as inlet air temperature, velocity, and agitator rotational speed were feedback controlled to maintain a stable operation. All the operational variables measured were on-line monitored *via* personal computer, then stored on hard disk.

Powder Samples Table 1 lists powder samples used. Spherical particles made of crystalline cellulose (Celphere CP-203, 305 and 507, Asahi Chemical Industry Co. Ltd.) having three different sizes were used. For each experiment, 0.75 kg of the particles was fed into the fluidized bed before dampening. Here, water absorption potential means the ratio of water mass possibly absorbed by the particle to the particle mass. Over 100% shows that the particle can absolve water greater than the particle mass.

Method Before the drying experiment, spherical particles were dampened to $W=15$ wt% using an IR moisture control system[2,3] in an agitation fluidized bed. After being dampened, drying experiments started under various operating conditions. This moisture control aimed to obtain particles having the same initial moisture content. Dampening time was 15 min, which was sufficient to dampen the particles uniformly.

During the drying experiments, a few grams of particles were periodically sampled out and dry basis (solid basis) moisture content was calculated using a shelf dryer to measure the weight decrease (=equivalent to water content). Temporal change in the moisture content was used to calculate the drying rate. Eventually, the heat transfer coefficient was obtained by using

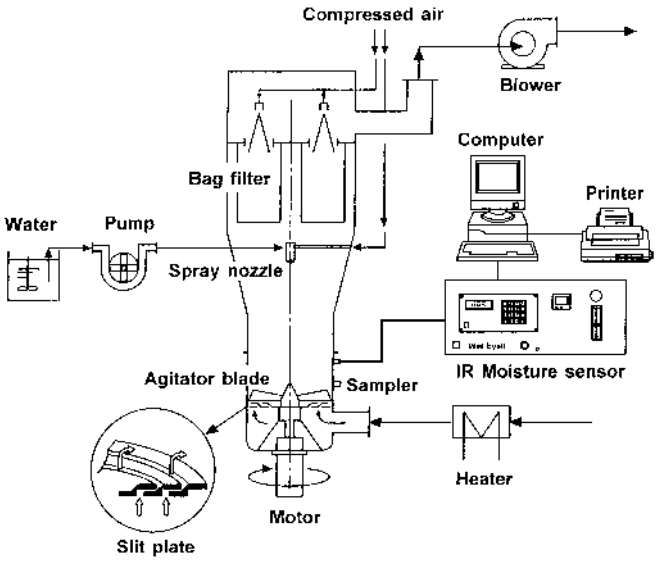

Fig. 1. Schematic Diagram of Agitation Fluidized Bed Used

* To whom correspondence should be addressed.

Table 1. Properties of Powder Samples Used

Properties		CP-203	CP-305	CP-507
Mass median diameter	[μm]	217	365	600
Geometric standard deviation	[—]	1.21	1.23	1.27
True density	[kg/m^3]	1484	1484	1484
Bulk density	[kg/m^3]	813	926	934
Water absorbing potential	[%]	100	110	100

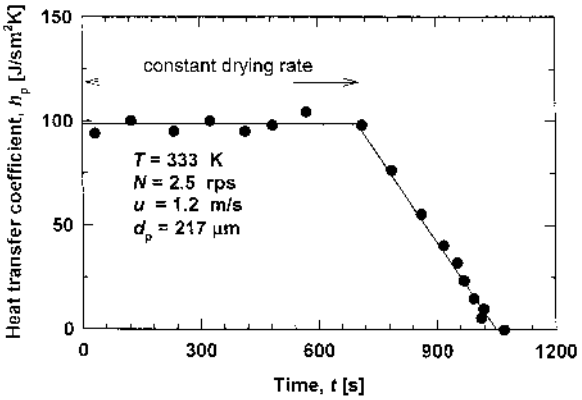

Fig. 2. Temporal Change in Drying Rate

the drying rate. In this experiment, the heat transfer coefficient at the constant drying rate period was measured as shown in Fig. 2. In this figure, T, N, u and d_p mean inlet air temperature, agitator rotational speed, inlet air velocity and mass median diameter of the used particles, respectively.

Results and Discussion

Temperature Distribution of Fluidizing Bed Before starting the drying experiments, the temperature distribution inside the particle beds was investigated.

Figures 3 and 4 show the axial and radial temperature distributions inside the particle beds, respectively. Seen from Fig. 3, there was a large temperature gradient near the air distributor, followed by a constant air temperature distribution at a vertical distance greater than 20 mm above the air distributor. The air reached thermal equilibrium soon after the air passed through the distributor. This implied that the mixing of air and particles was very good and the thermal energy supplied from the heated air to the particles was assumed to be totally consumed to dry the water inside the particle. Seen from Fig. 4, the air temperature difference between the center and the wall was less than 1 K. Thus the radial air temperature distribution could be neglected. In addition to these temperature distributions, the similar results were also observed when the operating condition was varied.

As a result, the heat transfer inside the agitation fluidized bed was found to be very good. In the later experiments, we decided to measure the air temperature after its equilibrium in case of calculating the heat transfer.

Heat Transfer Coefficient between Air and Particles Let the surface temperature of particle is equal to wet bulb temperature, T_w. Heat balance between air and particles can thus be written as

$$M_p \cdot R_c \cdot \gamma_w = h_p \cdot A \cdot (T - T_w) \quad (1)$$

where M_p [kg-solid] is the mass of particles, R_c ($=\Delta W/\Delta t$) [kg-water/kg-solid·s] the drying rate at the constant drying

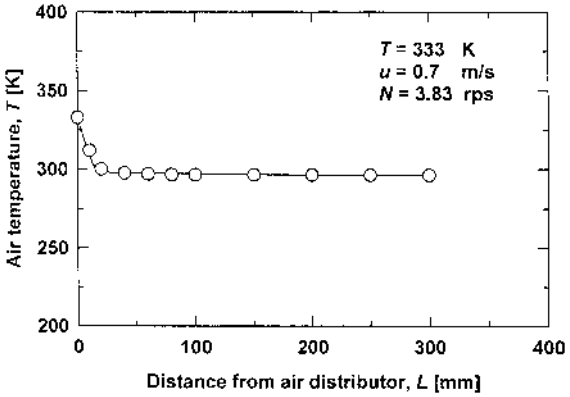

Fig. 3. Axial Temperature Distribution

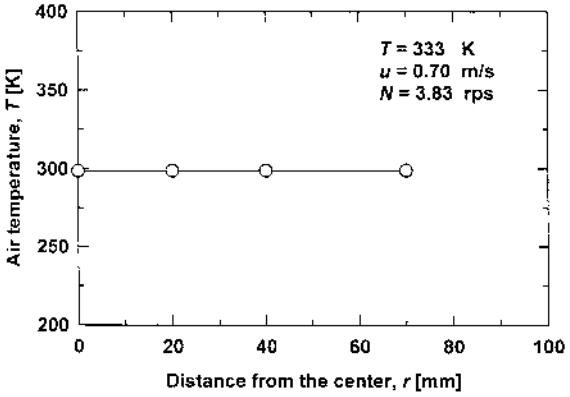

Fig. 4. Radial Temperature Distribution

period, γ_w [J/kg-water] the latent heat of evaporation at T_w [K], h_p [J/sm^{2}K] the heat transfer coefficient between air and particles, and A [m^2] the interfacial surface area between air and particles, respectively. Both sides of the Eq. 1 thus show the energy transfer speed needed for water evaporation.

In the preliminary study, it was confirmed that the air temperature decreased rapidly and reached a thermal equilibrium soon after the air passed through the distributor. Thus the temperature difference between T and T_w was measured when the air reached thermal equilibrium with the granules.

In Eq. 1, the air–particle interfacial area is calculated by the following equation on the basis of assumptions that particle shape is spherical and particle surface area contributes effectively to heat transfer.[10] In addition to these assumptions, particle diameter is kept constant regardless of the absorbed moisture content within this experimental condition;

$$A = \frac{6(1-\varepsilon)V}{d_p} \quad (2)$$

where V and d_p show the mean volume of fluidized bed and the particle diameter, respectively. In addition, ε expresses a void fraction[12] calculated by

$$\varepsilon = 1 - \frac{M}{\rho_w A_f L_f} \quad (3)$$

where, M, A_f and L_f indicate particle wet mass, the cross sectional area of the fluidized bed column and height of fluidized particle bed, and ρ_w denotes the granule wet density,

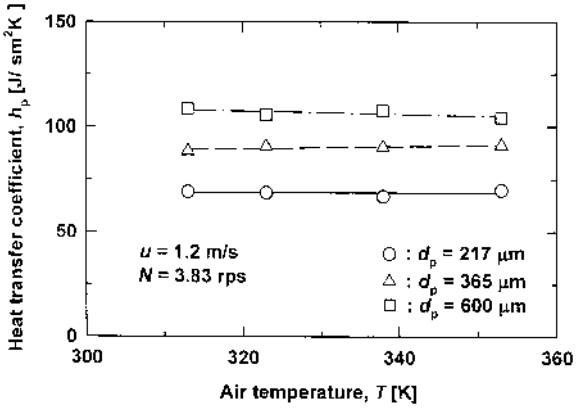

Fig. 5. Effect of Air Temperature on Heat Transfer Coefficient between Air and Particles

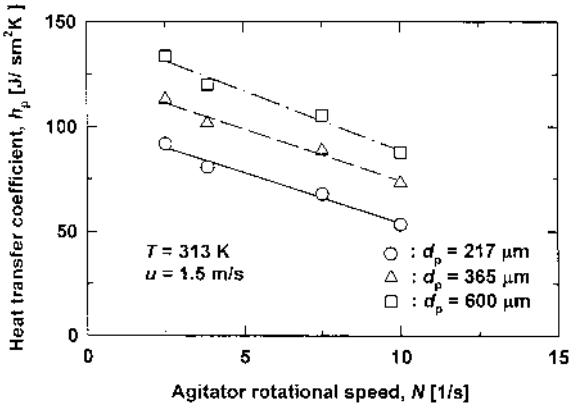

Fig. 6. Effect of Agitator Rotational Speed on Heat Transfer Coefficient between Air and Particles

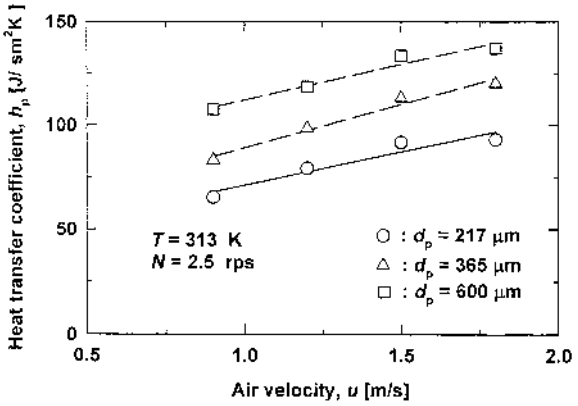

Fig. 7. Effect of Air Velocity on Heat Transfer Coefficient between Air and Particles

which has been measured using a powder tester (Hosokawa Micrometritics Laboratory).

Figures 5, 6 and 7 indicate the effect of air temperature, agitator rotational speed and air velocity on the heat transfer coefficient, respectively.

As can be seen from Fig. 5, the heat transfer coefficient is almost a constant value regardless of the air temperature. However, the heat transfer coefficient decreased with the agitator rotational speed (Fig. 6), while it showed an increase with the air velocity (Fig. 7). When the rotational speed was high, particles received strong centrifugal force from the

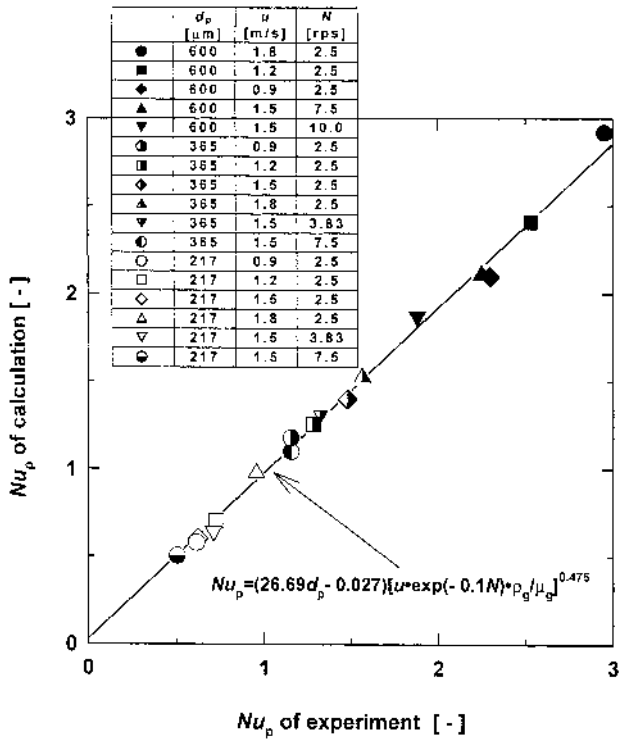

Fig. 8. Empirical Equation to Predict Heat Transfer Coefficient

blade, and they condensed near the wall. In such a case, since particles formed a softly condensed mass, the interfacial effective surface area decreased, resulting in a decrease in the drying rate. On the contrary, when the agitator rotational speed was slow or air velocity was high, particles were well fluidized due to the small centrifugal force. When particles were independently and intensely fluidized, the interfacial effective surface area increased, leading to an increase in the drying rate.

In all cases, larger particles showed a larger heat transfer coefficient. This was thought to be the effect of aggregation; small particles tended to form a soft aggregation due to the adhesion force between the particles such as liquid bridge force or electrostatic force. If small particles form a soft aggregation, the effective interfacial area between air and particles will decrease, leading to a decrease in the heat transfer coefficient. On the other hand, the large particles are difficult to form an aggregation due to their large mass. These particles could move independently in the fluidizing air, showing a large heat transfer coefficient.

From the data seen from Figs. 6 and 7, the heat transfer coefficient seemed to have almost linear relationships with air velocity, agitator rotational speed and particle size, and an empirical equation will be proposed to describe the effects of these parameters on the heat transfer coefficient.

Prediction of the Heat Transfer Coefficient An empirical equation for particle Nusselt number, Nu_p, is proposed to predict the heat transfer between air and particles under various operating variables and particle sizes.

$$Nu_p=(26.96d_p-0.027)[u\cdot\exp(-0.1N)\cdot\rho_g/\mu_g]^{0.475} \quad (4)$$

where, ρ_g and μ_g are the density and viscosity of air, respectively.

Table 2. Difference between the Heat Transfer Coefficient Calculated and Experimental

Run. No	Mass median diameter [μm]	Geometric standard deviation [—]	$h_{p,cal}$ [J/s m^{2}K]	$h_{p,exp}$ [J/s m^{2}K]	$(h_{p,exp}-h_{p,cal})/h_{p,exp}$ $\times 100$ [%]
1	368	1.94	83.44	97.93	14.73
2	352	1.54	79.49	87.12	8.75
3	343	1.37	58.88	63.85	7.79

Figure 8 describes the relationship between Nu_p of calculated and of experiments. There was a fairly good correlation between the two data. By using the empirical equation, the heat transfer could be predicted with high accuracy.

To confirm the validity of the proposed equation, we tried to measure the heat transfer coefficient of the particles having a wide size distribution and to compare the coefficient with the one from the empirical equation. Here, in order to calculate the interfacial surface area of the particles having a wide size distribution, we used the following equation.

$$A=\sum_{i=1}^{9}\frac{6M_{pi}}{\rho_p \cdot d_{pi}} \tag{5}$$

In Eq. 5, i means the number of meshes used for measuring the particle size distribution and M_{pi} and d_{pi} showed the weight of the particles on the i-th mesh and representative diameter of the mesh, respectively (9 meshes of different seizes were used for sieving).

Table 2 lists the particle size distribution of the particles and their experimental and calculated heat transfer coefficients. Calculated heat transfer coefficients were a little bit smaller than the ones from the experiments. It was considered that the void fraction decreased due to the wide particle size distribution. However, since both data were in good agreement, the proposed empirical equation could be used for the particles having a wide size distribution.

As a result, we could analyze the heat transfer coefficient between air and particles in agitation fluidized bed. And our proposed empirical equation could be used to predict the heat transfer coefficient under various operating conditions and particles size distribution.

Conclusions

In this paper, experiments were carried out to analyze the heat transfer coefficient between air and particles in an agitation fluidized bed drying. The effects of the operating conditions and particle diameter on the heat transfer coefficient were clarified. Also, an empirical equation was proposed to predict the heat transfer coefficient under various operating conditions and particle size. The empirical equation was in good agreement with the experimental results. It was also confirmed that this equation could be used for particles having a wide size distribution.

References

1) Takei N., Unosawa K., Takemura Y., *Proc. of Sixth International Symposium on Agglomeration*, 532—537, Nagoya, Japan (1993).
2) Watano S., Yamamoto A., Miyanami K., *Chem. Pharm. Bull*., **42**, 133—137 (1994).
3) Watano S., Morikawa T., Miyanami K., *J. Chem. Eng. Jpn*., **28**, 171—178 (1995).
4) Watano S., Sato Y., Miyanami K., *Powder Technol*., **90**, 153—159 (1997).
5) Davidson J. F., Harrison D., "Fluidization," Academic Press, London, U.K., 1971.
6) Kunii D. Levenspiel O., " Fluidisation Engineering," Butterworth-Heinemann, London, U.K., 1991.
7) Chandran A. N., Rao S. S., Varma Y.B.G., *AIChE. J*., **36**, 29—38 (1990).
8) Suzuki K., A. Fujigami R., Yamazaki R., Jinbo G., *J. Chem. Eng. Jpn*., **13**, 117—122 (1980).
9) Thomas P. P., Varma Y. S. G., *Powder Technol*., **69**, 213—222 (1992).
10) Watanabe T., Chen Y., Naruse I., Hasatani M., *Kagaku Kogaku Ronbunshu*, **18**, 601—606 (1992).
11) Watano S., Yeh N., Miyanami K., *J. Chem. Eng. Jpn*., **31**, 908—913 (1998).
12) Watano S., Fukushima T., Miyanami K., *Chem. Pharm. Bull*., **44**, 572—576 (1996).